



**Queensland University of Technology**  
Brisbane Australia

This may be the author's version of a work that was submitted/accepted for publication in the following source:

Quince, Zachery, Alonso-Caneiro, David, Read, Scott A., & Collins, Michael J.

(2021)

Quantitative compressive optical coherence elastography using structural OCT imaging and optical palpation to measure soft contact lens mechanical properties.

*Biomedical Optics Express*, 12(12), pp. 7315-7326.

This file was downloaded from: <https://eprints.qut.edu.au/227199/>

© © 2021 OSA - The Optical Society. All rights reserved.

Users may use, reuse, and build upon the article, or use the article for text or data mining, so long as such uses are for non-commercial purposes and appropriate attribution is maintained. All other rights are reserved.

**Notice:** *Please note that this document may not be the Version of Record (i.e. published version) of the work. Author manuscript versions (as Submitted for peer review or as Accepted for publication after peer review) can be identified by an absence of publisher branding and/or typeset appearance. If there is any doubt, please refer to the published source.*

<https://doi.org/10.1364/BOE.441547>



# Quantitative compressive optical coherence elastography using structural OCT imaging and optical palpation to measure soft contact lens mechanical properties

ZACHERY QUINCE, \*  DAVID ALONSO-CANEIRO, SCOTT A. READ, AND MICHAEL J. COLLINS

*Queensland University of Technology (QUT), Centre for Vision and Eye Research, School of Optometry and Vision Science, Kelvin Grove, Queensland, Australia*

\*[zach.quince@hdr.qut.edu.au](mailto:zach.quince@hdr.qut.edu.au)

**Abstract:** In this study, the principle of ‘optical palpation’ was applied to a compression optical coherence elastography (OCE) method using spectral domain optical coherence tomography (OCT). Optical palpation utilizes a compliant transparent material of known mechanical properties, which acts as a stress sensor, in order to derive the mechanical properties of a sample material under examination. This technique was applied to determine the mechanical properties of soft contact lenses, with one lens being used as the compliant stress sensor and the other as the sample under investigation to extract the mechanical properties. This compliant stress sensor allowed for the stress of the compression to be measured without the use of a force sensor. The strain of the materials was measured through an automatic boundary segmentation that tracks the material thickness (of the sensor and the sample) during compression through sequential structural OCT images. A total of five contact lens combinations were tested, using three separate commercially available contact lenses with unique mechanical properties. Various combinations of contact lens materials were used to further validate the technique. The Young’s modulus derived from this method was compared to nominal manufacturer’s values. Both accuracy and repeatability were assessed, with highly accurate measurements obtained, with a percentage difference between the nominal and experimentally derived Young’s modulus being less than 6% for all the tested combinations as well as providing a Young’s modulus that was not statistically significant different ( $p > 0.01$ ) to the nominal value. The results demonstrate the potential of optical palpation in OCE to accurately measure the mechanical properties of a material without the use of sophisticated electronics to capture the stress of the sample. These findings have potential to be translated into a method for tissue mechanical testing with ex vivo and in vivo clinical applications.

© 2021 Optical Society of America under the terms of the [OSA Open Access Publishing Agreement](#)

## 1. Introduction

Testing of tissue mechanical properties has traditionally required a destructive method and/or the use of an ex vivo sample. Tensile testing, for example requires the material to be pulled between two clamps, a technique that is not suitable for in vivo applications. Optical coherence elastography (OCE) offers an alternative as a nondestructive method for analysis of mechanical properties, which has great potential for biomedical applications and may be particularly applicable to measure the mechanical properties of the anterior tissues of the eye, since optical coherence tomography (OCT) is an imaging modality that has been widely used for ocular imaging [1]. There are multiple variations of OCE methods that can be used to determine the Young’s modulus or the elastic modulus of a material or tissue. OCE uses OCT to image the changes in a tissue or material in response to stress, and depending on the loading technique, different responses and mechanical properties can be extracted [1,2]. For example, phase-stabilized OCT instruments

can capture the phase information of a sequence of images from which small sub-pixel tissue displacement or surface wave propagation can be extracted. A transient response OCE method developed by Singh et al. [3], in which a non-contact air pulse imaging method was used to evaluate the changes in corneal elasticity after corneal crosslinking (CXL). A localized air pulse (inducing a 1 micron displacement) was applied to ex vivo human donor corneas and the resulting propagating wave was measured by a phase-stabilized swept source OCT instrument. Through this method, the Young's modulus of the tissue was measured through knowledge of the materials wave velocity, Poisson's ratio and density.

Clinically available OCT instruments, such as the commonly used spectral domain OCT (SD-OCT) and swept source OCT (SS-OCT) instruments, do not typically provide access to the phase information from their OCT data. Thus, the use of a phase tracking image analysis is not viable with these instruments and an alternative loading method is needed, such as compressive OCE. Static compressive loading can cause a thickness/movement change in a material or tissue, which can be quantified by analyzing sequential OCT images using a bulk volume change. Through the analysis of these images, the strain can be extracted by quantifying the changes in the sample during loading, however, to calculate the Young's modulus of the material, knowledge of the stress is required. The stress, which is the applied force over the surface area of the material during loading, can be challenging to determine, especially for in vivo studies, as it is challenging to integrate force sensors into the OCE setup without compromising the integrity of in vivo measurements. Ford et al. [4] used compression OCE to image tissue mimicking phantoms and ex vivo corneal tissue and showed that edematous corneas exhibited greater strain than normal and CXL corneas. De Stefano et al. [5] developed a depth-dependent OCE method, that used a custom-built OCT to measure the displacement caused by a flat lens controlled by a precision linear displacement stage, incorporating a highly sensitive force sensor. The study used a speckle tracking algorithm to measure the displacement of the anterior and posterior cornea under different anatomical states. Whilst Young's modulus was not reported, the force/displacement relationship was shown as a linear slope defined by the value 'k'. Previously, we have used a similar compression OCE method with an integrated, fully calibrated piezoresistive-based force sensor to measure the mechanical properties of soft contact lens materials [6]. The bulk thickness change of the contact lenses were measured using an automatic boundary segmentation of the anterior and posterior lens surfaces, from which the strain could be extracted. The stress was derived by using the force sensor and capturing the contact area from an en face scanning laser ophthalmoscope (SLO) image. Using this setup, the mechanical properties of a range of soft contact lens materials could be accurately extracted. Despite the potential of compressive OCE methods to characterize material and tissue biomechanics, the measurement of the stress during the loading of the tissue can be challenging, so an alternative method without the need for sophisticated force sensor systems, which may be also viable for in vivo testing, is desirable.

Kennedy et al. [7] proposed a method of calculating the stress of a material under loading indirectly through OCE imaging, using a method that was termed 'optical palpation'. Optical palpation incorporates a compliant material between the material under examination and a compression plate. The compliant material or 'stress sensor' should have well-defined mechanical properties, from which the local stress can be calculated using the known Young's modulus and the induced strain. This stress was then mapped onto the material under investigation to measure the Young's modulus of the material. The authors validated the method with a range of materials, including two sets of custom-made tissue mimicking phantoms made out of silicone with known mechanical properties and ex vivo human breast tissue, demonstrating that optical palpation OCE was able to accurately determine the stress using a compliant layer between the compression plate and the material, without the use of a stress sensor. Later, this technique was applied to human breast tissue to map the elasticity of the tissue sample [8], providing an elasticity map of malignant human breast tissue to highlight regions of pathology. Although

a number of studies have integrated optical palpation into OCE methods [8–10], to date, the method of optical palpation has not been used for the measurement of mechanical properties of soft contact lenses. Previous optical palpation-based methods have utilized phase-sensitive detection, which is not possible using clinical, commercially available OCT devices, and also requires the application of complex strain detection algorithms.

This study therefore aimed to develop and apply the optical palpation principle to compression OCE to measure the mechanical properties of soft contact lenses using the intensity/structural images from a commercial OCT instrument. Soft contact lenses are particularly suitable for this application and could be used as a stress sensor in future clinical applications due to their: relatively linear stress/strain relationships at low strains (< 15%), well documented mechanical properties, and their suitability for being imaged with OCT. The mechanical properties of soft contact lenses are important contributors to the in vivo comfort of lenses and their effects on ocular anatomy and physiology [11,12]. Soft contact lenses are designed to conform to the surface of the eye and to be worn comfortably in vivo with minimal impact on the physiology of the underlying ocular tissues and so this study also provides the foundations to further develop an OCE technique to characterize in vivo anterior eye tissue mechanical properties in the future.

## 2. Methodology

This section provides a detailed description of the hardware and software components that were designed and evaluated in this study. It also describes the theoretical principles behind the technique and the materials used for testing. Finally, the statistical methods used to analyze the results are described.

### 2.1. Theoretical principles

This study aimed to use compression OCE and adapt the ‘optical palpation’ principle to measure the mechanical properties (Young’s modulus) of soft contact lenses. Part of the OCE methodology follows a previously presented study [6], which also characterized the mechanical properties of soft contact lenses. However, while the previous work used a force sensor to directly measure the force applied to compress the contact lens and determine the stress (through knowledge of the force/area relationship), this study uses a stress sensor (i.e. a compliant layer of known mechanical properties) and applies the principles of optical palpation instead to characterize the stress indirectly. A spectral domain OCT (SD-OCT) was used to capture high resolution OCT images of the contact lenses during loading. The stress sensor used in this experiment was also a soft contact lens, such that the system being analyzed was two contact lenses on top of each other. The contact lenses were selected due to their well-known mechanical properties and their ability to be imaged with OCT. The contact lenses also easily conform to the shape of the anterior eye surface, thereby creating the opportunity for future in vivo applications to investigate this OCE methodology.

The compression OCE method works by deriving the stress of the sensor through knowledge of the Young’s modulus of the sensor and the strain under loading, which is then mapped onto the contact lens under investigation (sample) such that the Young’s modulus of the sample can be determined through the resultant strain and stress map. Each lens will have the volumetric strain determined by the bulk thickness change calculated through analysis of volumetric OCT scans of the sample, using an automated boundary segmentation method. The strain of the contact lenses ( $\epsilon$ , unitless) can be determined through (1). It should be noted that only axial strain (axial thickness change) is being measured during this experiment.

$$\epsilon = \frac{L_{PL} - L_C}{L_{PL}}. \quad (1)$$

Where,  $L_{PL}$  is the ‘pre-loaded’ thickness of the contact lens during the pre-load compression and  $L_C$  is the ‘compressed’ thickness of the contact lenses during compression, both in  $\mu\text{m}$ . To determine the stress ( $\sigma$ , MPa) of the sensor (2) is used.

$$E = \frac{\sigma}{\varepsilon}. \quad (2)$$

Where E is the Young’s modulus (MPa). Based on the optical palpation principle, the stress derived by (2) from the compliant layer (4) was used to analyze the contact lens combination, assuming (3) stands:

$$\sigma_1 = \sigma_2 \quad (3)$$

$$E_1 \varepsilon_1 = E_2 \varepsilon_2 \quad (4)$$

where  $E_1$  and  $\varepsilon_1$  are the Young’s modulus and the strain of the compliant layer, while  $E_2$  and  $\varepsilon_2$  are the Young’s modulus and the strain of the contact lens under investigation. Following similar principles to our previous study [6], the proposed method has several underlying assumptions including: the contact lens is assumed to be isotropic and will undergo a uniform stress, the stress is distributed evenly throughout both lenses, the force is considered to be applied uniaxially with no surface friction such that there are no volume changes and contact lens viscoelastic behavior and refractive index change under compression are considered negligible.

An example of the analysis pipeline is as follows. Using two sequential images, the change in the two-contact lens thickness (sensor/sample), the strain of both contact lenses was derived through (1). The stress of the compliant sensor was then determined by using (2) and the manufacturers published Young’s modulus of the sensor. Since stress in both contact lenses is assumed to be equal (as per (3)), this stress is then applied to the contact lens under investigation and using (2) the Young’s modulus of the contact lens under investigation is calculated.

## 2.2. Hardware

The hardware setup consists of two main parts, that is the imaging side and the sample side Fig. 1. The sample side contains the material being tested together with the stress sensor and the Digimatic micrometer head series 164 (Mitutoyo, Aurora, IL). The micrometer is used to precisely move the sample as it allows for 1  $\mu\text{m}$  displacement per dial-rotation. The imaging head of the Spectralis OCT instrument (Heidelberg Engineering GmbH, Germany) has a 3D printed mount that holds a glass plate, which acts as a compression plate. The commercial OCT instrument uses a super luminescent diode (SLD) operating at a central wavelength of 870 nm. The axial range of the OCT is 1.9 mm (in tissue).

The contact lenses were imaged using a volumetric scanning protocol (approximately 8.22 mm horizontal and 2.78 mm vertical) with the OCT instrument’s anterior segment lens attachment. The volumetric scan comprised a total of 11 B-scans (278  $\mu\text{m}$  separation between B-scans) and each B-scan contained 768 A-scans. The volumetric scan takes approximately three seconds to capture all 11 B-scans. The OCT images have a transversal and axial resolution of 10.8  $\mu\text{m}$  x 3.87  $\mu\text{m}$  per pixel, respectively. During the lens testing, two sets of images were captured: pre-load images and compression images. A pre-load of approximately 1% strain was applied for the initial set of images to remove any induced arc on the contact lens and to minimize any intensity flares that may be present in the images. For the compression images, the contact lenses were compressed until there was a noticeable change in the B-scan that corresponded to approximately a 10% change of the lens thickness, which could be roughly estimated from the lens thickness and the rotation/displacement on the micrometer head. The contact lenses were compressed for a period of 3-5 seconds.

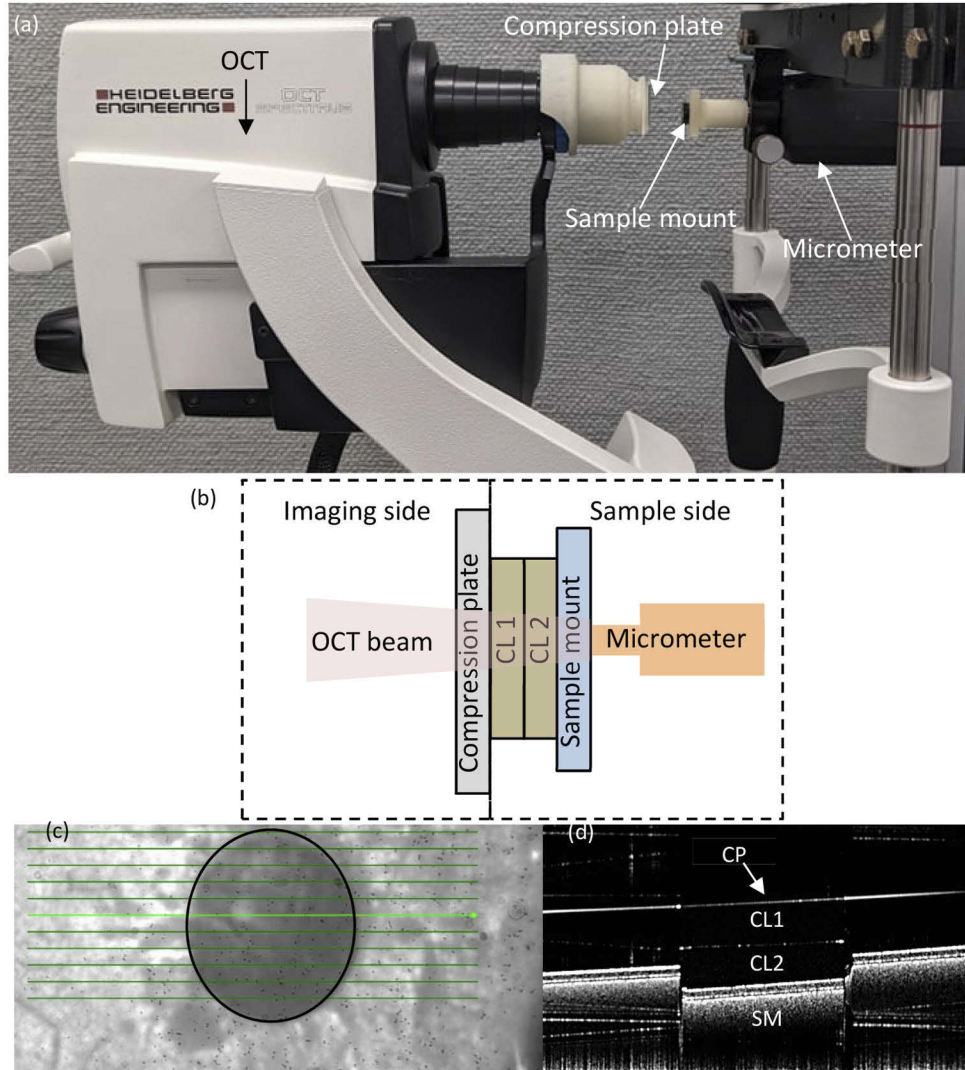


**Fig. 1.** Schematic diagram of the static compression OCE methodology, showing the experimental setup (a), a diagram of the setup under loading (b). (c) is an SLO image of the en face image of the contact lens (outlined) showing the scanning protocol of the experimental setup. (d) shows a single OCT B-scan which corresponds to the highlighted green line in the SLO image (image contrast has been increased for visualization purposes). CP is the compression plate, SM is the sample mount, CL1 represents the contact lens under examination, which has a higher Young's modulus, while CL2 represents the contact lens being used as the compliant stress sensor.

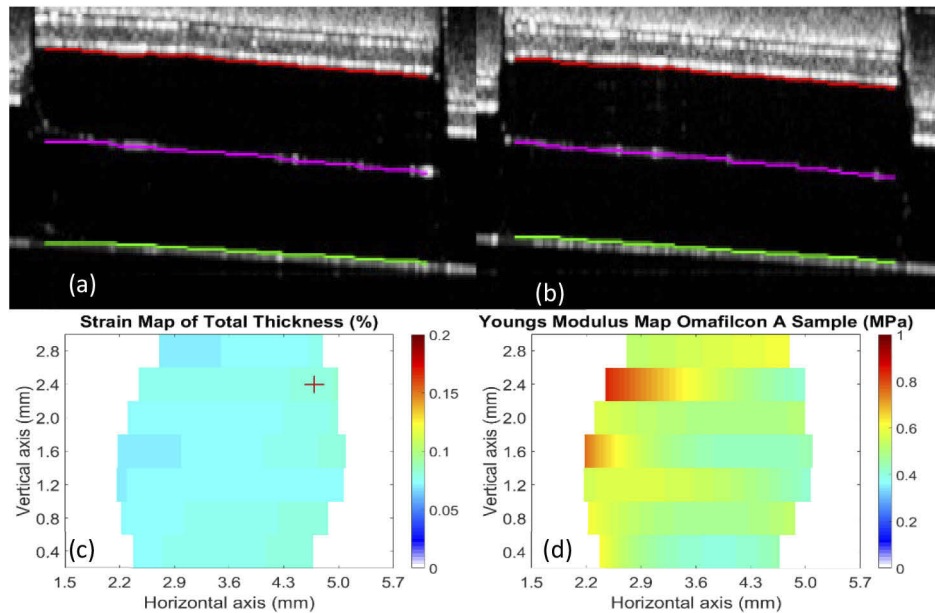


**Fig. 2.** (a) Pre-load and (b) compression B-scan image for the same contact lens combination and the approximate same cross-section. Red line represents the posterior surface of CL1 (contact lens under investigation). Purple line represents the mean contact boundary between the two contact lenses, average of the anterior surface of CL1 and the posterior surface of CL2. Green line represents the anterior surface of CL2 (contact lens used as a stress sensor). (c) Image of the total strain for the combination of CL 1 and CL 2. The + red symbol represents the selection point for the Young's modulus. (d) is an image of the Young's modulus map of the contact lens under examination (CL 1) measured in MPa.

### 2.3. Software

To determine the Young's modulus of the contact lens that is under examination, knowledge of the stress and strain values are required. The strain, which is the change in thickness divided by the original thickness values (1), of both contact lenses can be determined using an automatic segmentation code based on a previously developed graph-search method for OCT image segmentation [6,13,14], which was adapted to extract the 3 boundaries of interest from each of the OCT images captured in this study. This code uses a graph-search method with dynamic processing to determine the anterior and posterior surfaces of both contact lenses. For all B-scan images the automatic segmentation was applied, and an observer verified the integrity of the segmentation and corrected any boundaries errors, if needed. Due to the highly variable reflectivity profile of the middle layer (surfaces between the stress sensor and lens under examination), the average of the anterior and posterior boundary positions for each lens was calculated and used as the boundary. All 11 of the captured B-scans in each volume were segmented for both the pre-load and compression images. Due to the optical distortion produced by the change in the refractive index of the contact lenses material, a correction method was applied to compensate for the specific refractive indices of the materials [15,16]. The refractive indices of the different materials are given in Table 1, extracted from the manufacturer's specifications.

The analysis procedure can be divided into several steps. The first is to determine the strain map of both contact lenses, which is the thickness change between conditions (pre-load and compression) divided by the pre-load contact lens thickness. Figure 2(a) & 2(b) show the central

B-scan for the pre-load and compression conditions, respectively. A compression of about 8% in both contact lenses was recorded, it is worth noting this image represents only a single B-scan out of the 11 comprising the volumetric set. Once the strain is determined, the Young's modulus of the compliant layer is applied to the strain through (2) and the stress can then be calculated. The stress map is then applied to the strain map of the contact lens under investigation to determine the Young's modulus map (Fig. 2(d)). From this Young's modulus map (Fig. 2(d)) a single point needs to be extracted so the values can be compared the nominal values to determine the accuracy of the methodology. For this point the strain map of both materials (Fig. 2(c)) as a whole is assessed and the maximum strain is calculated using the thickness changes measured by the red and green segmented lines (Fig. 2(a) & (b)). In a situation where there are multiple maximum strain points, a manual examination was conducted with the largest area of maximum strain used. Each of these points were examined to ensure that the segmentation had no errors (e.g. the presence of small localized intensity flares in the OCT image that caused the segmentation algorithm to incorrectly track the wrong group of pixels), and if none of these points were suitable, then the middle of the images was typically chosen.

#### 2.4. Materials

Three different commercially available contact lens materials were tested: each having a different Young's modulus and water content. Table 1 provides a summary of the contact lens materials and their properties. The contact lens material was cut into a circle with an approximate radius of 1.5 mm from the center of the lens. All the tested lenses had the same back vertex power of +6.00 Diopters. In order to assess the repeatability of the method, three of each lens combinations were tested, and all lens-combinations were imaged four times. Thus, capturing measurements both within-lens and across lenses of the same material/combination.

**Table 1. Selection of Contact Lens Materials Used<sup>a</sup>**

Material	Water content (%)	Base curve (mm)	Diameter (mm)	Thickness ( $\mu\text{m}$ ) [6]	Refractive index	Young's modulus (MPa) [17]
Omafilcon A	62	14.2	8.7	216	1.39	0.40
Senofilcon A	38	14.0	8.4	148	1.42	0.73
Lotrafilcon B	33	13.8	8.4	162	1.42	1.20

<sup>a</sup>Water content, base curve and diameter were extracted from manufacturer specifications. Central thickness measurements taken from OCT imaging using a +6.00 D lens, with no compression on the lens and adjusting for the specific material refractive index.

There are a range of factors that can influence the mechanical properties of contact lenses [11], [18]. Soft contact lenses contain water, thus requiring consistent hydration, to minimize variations in their mechanical properties [19]. To avoid changes in material properties due to dehydration, between measurements the lenses were immersed in a sterile saline solution (sodium chloride and potassium phosphate monobasic) for a period of at least two minutes before the lens was imaged again. The contact lens with higher elastic modulus, which was the contact lens that was under examination during testing, was immersed in a high molecular fluorescein sodium dye (0.5 mg) for a period of 5 minutes to give a change in color, so it could be distinguished from the other lenses being imaged. The temperature of the lens has been shown to be a key factor affecting mechanical properties [18]. The experiment was conducted in the same room and the temperature and humidity of the room were controlled. The average (mean  $\pm$  standard deviation) temperature in the measurement room during testing of the lenses was  $23 \pm 1$  °C, and the average humidity was  $53 \pm 5\%$ .

Given the contact lens material was used as a stress sensor and testing material, a criterion was defined to make sure that the lens combinations used would provide reliable measurements.



Both contact lenses would have to be under less than 15% strain, as this was determined to be a conservative upper limit of the linear region of the stress/strain curve for the lens materials. If the strain of the softer contact lens (stress sensor) is set to 15% and then the strain of the contact lens under investigation was estimated, using Eq. (4). If the estimated strain of the contact lens under investigation was any less than 5% then the lens-combination was deemed invalid. This lower limit on the strain was determined based upon the accuracy of the segmentation and the axial resolution of the OCT instrument. In other words, a strain below 5% may result in contact lens variation that cannot be accurately measured by the imaging and image analysis method. For example, when applying the criteria to a Lotrafilcon B and Omafilcon A material combination, the strain of Omafilcon A strain was set to 15% and the corresponding Lotrafilcon B strain was 4.49%. Thus, this combination was deemed not viable, the final five tested lens combination can be seen in Table 2.

### 2.5. Statistical analysis

The statistical analysis was divided into two sections: the repeatability assessment of the proposed method and the performance evaluation (accuracy) of the method. To assess the repeatability of the method, three different metrics were calculated including: the within trial standard deviation ( $S_w$ ), the coefficient of variation (CV) and the coefficient of repeatability (COR). The standard deviation was calculated using a one-way analysis of variance (ANOVA). The COR was then determined based on the  $S_w$  to further quantify the repeatability of the proposed technique for each of the combination of lenses [20]. To allow comparisons between the contact lens materials, the CV was calculated, which is the standard deviation normalized to the mean of the results. The performance was assessed through a comparison of the mean results provided by the method with the nominal values given by the manufacturer, through a one sample t-test. Given that this analysis involved 5 repeated t-tests, an alpha value of 0.01 was considered statistically significant, to account for the multiple comparisons.

## 3. Results and discussion

This study focused on examining the viability of using a compliant stress sensor in the application of compression OCE, removing the need for an additional electronic force sensor. The repeatability of the method was assessed using several metrics (Table 3). The within trial standard deviation ( $S_w$ ) showed that there was more spread in the results while testing lens combinations with different materials. The  $S_w$  was found to be below 0.029 MPa for combinations of the same materials, and to be above 0.133 MPa for combinations of different materials. Similarly, the COR was below 0.6 MPa for all lenses and the lowest values were recorded for lenses measured with the same material combination. Young et al. [21] reported a COR of between 0.04 and 0.30 MPa for a range of materials, which is comparable to the current study. Whilst Kim et al. [17] reported a COR of between 0.02 and 0.08 MPa which again is within the range of values of the current study. Both studies used a tensile method to determine the mechanical properties. These metrics show that the repeatability of this method is comparable to other methods used to calculate the Young's modulus of soft contact lenses. The CV was measured for all lenses, which is a metric to capture the variability normalized to the mean. The CV for Lotrafilcon B measured using a Senofilcon A lens as stress sensor was 16.195% in comparison to being measured using a Lotrafilcon B material with a CV of 2.045%.

A statistical analysis was performed to examine the performance of the developed method. Five material combinations were tested, each of which had three different pairs and a total of four repetitions each (twelve trials in total for each lens combination). The standard deviation was calculated for each of the three repeat combinations, as well as overall mean of the combination. The percentage differences between the mean values and the nominal values were also calculated (Table 2).

**Table 2. Young's Modulus of Five Contact Lens Materials Tested (MPa)<sup>a</sup>**

Stress sensor material	Tested material	Trial 1	Trial 2	Trial 3	Mean	PD (%)
Omafilcon A	Omafilcon A	0.423 ± 0.011	0.431 ± 0.027	0.423 ± 0.036	0.426 ± 0.027	6.238
Senofilcon A	Senofilcon A	0.714 ± 0.016	0.741 ± 0.007	0.734 ± 0.014	0.729 ± 0.013	0.077
Lotrafalcon B	Lotrafalcon B	1.213 ± 0.034	1.220 ± 0.034	1.187 ± 0.015	1.207 ± 0.029	0.777
Omafilcon A	Senofilcon A	0.734 ± 0.018	0.703 ± 0.027	0.735 ± 0.054	0.724 ± 0.036	0.809
Senofilcon A	Lotrafalcon B	1.241 ± 0.137	1.215 ± 0.188	1.093 ± 0.237	1.183 ± 0.192	2.400

<sup>a</sup>The estimate for each lens is the average of four repeated measurement trials with the mean ± standard deviation shown. The standard deviation shown for the mean is the 'within lens' metric derived from the ANOVA. PD = percentage difference between the mean value and the manufacturers value.

**Table 3. Repeatability Analysis<sup>a</sup>**

Stress sensor material	Tested material	S <sub>w</sub> (MPa)	COR (MPa)	CV (%)
Omafilcon A	Omafilcon A	0.027	0.074	6.238
Senofilcon A	Senofilcon A	0.013	0.036	1.803
Lotrafalcon B	Lotrafalcon B	0.029	0.080	2.405
Omafilcon A	Senofilcon A	0.133	0.101	5.029
Senofilcon A	Lotrafalcon B	0.192	0.531	16.195

<sup>a</sup>Sw = within trial standard deviation, COR = the coefficient of repeatability, and CV = the coefficient of variation.

All the five tested combinations showed that the Young's modulus determined from our experimental method was not statistically significantly different from the manufacturer's value ( $p > 0.01$ ). The percentage difference of all combinations with the exception of Omafilcon A/Omafilcon A and Senofilcon A/Lotrafalcon B were lower than 1%, showing very close agreement with the manufacturer's data. Interestingly these results suggest that the proposed method may be more accurate than the one presented in our previous study [6], which integrated an electronic force sensor and reported percentage differences with the manufacturer values of Young's modulus ranging from 6.04% for Lotrafalcon A to 16.77% for Omafilcon A. This could be due to the electronic sensor having an error of up to 5% of the output voltage, which was proportional to the force recorded. This force was used to find the stress of the contact lens. The higher percentage difference of 6.2% shown by the Omafilcon A/Omafilcon A combination, may be attributed to its softer material properties and higher water content, that may influence its performance. As the method uses thickness to measure strain, the softer the material, the smaller the change needs to be as the material will have a larger deformation under a lower force. This could be an indication that this softer and high-water content materials, may not be the optimal to use in future experiments. Future research with this method is required to determine the optimum sensor parameters in terms of both thickness and elasticity differences between the sensor and the sample to provide the most accurate measurements.

Figure 3 shows the mean Young's modulus recorded for the five contact lens combinations (test material and stress sensor material) tested along with the nominal values for the test material, demonstrating good agreement between the nominal and experimentally determined test material values. Through both the repeatability and performance analysis, the results of this study provide a proof of concept that a commercially available soft contact lens can be used as a stress sensor within an OCE setup for determining mechanical properties of material samples. Given the ability of soft contact lenses to be worn directly on the ocular surface, these results suggest the potential for the proposed method to be extended to the assessment of ocular tissue mechanical properties in future work. However, substantial developments in the methods would be needed for reliable in vivo clinical measurements, given the more complex mechanical properties of

ocular tissue, geometry and structural make up compared to contact lenses and the impact of other ocular physiological factors on these measures (e.g. intraocular pressure).

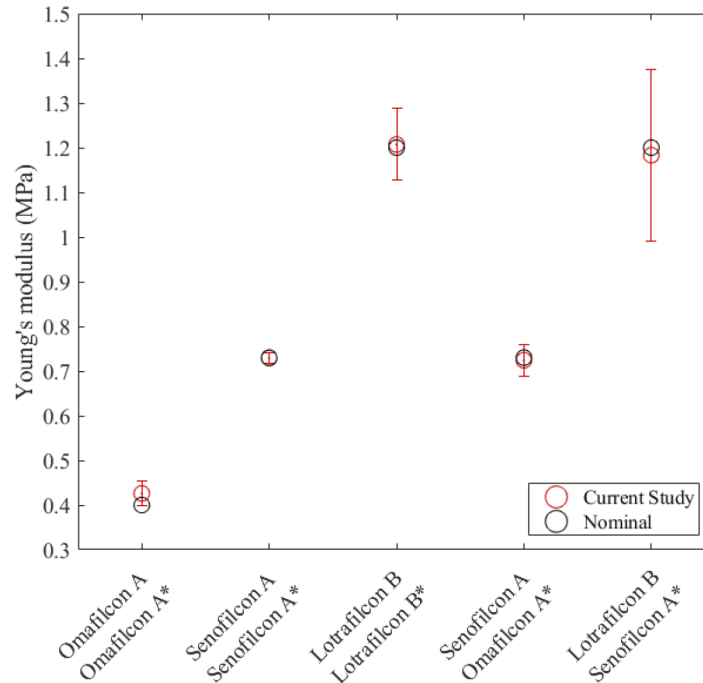


**Fig. 3.** Young's modulus of the five combinations of contact lenses used. The \* denotes the material that was used as the stress sensor.

This study is the first to use structural (intensity) OCT images to determine the strain in both the compliant sensor and the material under investigation. Compared to previous optical palpation methods requiring phase-sensitive detection, the proposed approach has several advantages, as well as some limitations. An advantage of the method described in this study is that the strain calculation method is more straightforward than a phase sensitive approach, with only the change in bulk thickness needing to be calculated. Our method also allows a relatively large strain to be introduced, which can be challenging for phase-based approaches. A limitation of our method is that since the bulk volume change is being calculated, the technique has a lower strain sensitivity than that of methods utilizing more advanced strain measurement approaches using phase sensitive OCT systems. Another limiting factor of our method is that the material being investigated is required to be transparent so the OCT beam can penetrate to the posterior surface of the material under examination. Currently, this study is measuring only the Young's modulus at an individual point in time and assuming that the response is purely linear. However, soft hydrogel materials and ocular tissues are viscoelastic and display a time dependent response to loading [22]. With the method presented, both the non-linear characteristics and the viscoelastic creep could be measured in future studies. There are several limitations of the technique and the materials used that should be considered, some of which have been discussed in previous work [6], including the strain sensitivity which was calculated to be approximately 1.25% (the change in strain caused by a single pixel shift with the thinnest material). This value decreases with increasing thickness of the sample. The contact lens material properties are assumed to be homogeneous across the tested section of the material. Similarly, contact lenses may exhibit viscoelastic behavior [22], however for the purpose of this study the material is assumed to behave in a linear manner. When the contact lenses are compressed, some movement is likely

to occur in both lateral and axial directions, yet in this study the lateral movement is assumed to be negligible. As this method relies on the force being transferred through the compliant layer and onto the material being investigated, it is assumed that it will be transferred without any loss due to friction and lateral movement of the material. Despite all of these potential limitations, the results suggest that the method provides a reasonable performance in terms of both repeatability and accuracy, so these potential limitations do not appear to have a major influence on the method. Further investigation into the application of this method for biological tissues is required to investigate how these assumptions hold for different tissue samples.

#### 4. Conclusions

In conclusion, this study was successful in applying the ‘optical palpation’ principle and using a compliant stress sensor in between a compression plate and a material to measure the stress of the compression. Through the use of commercially available OCT instrument, both the stress and strain of the material were determined and the subsequent Young’s modulus of a range of contact lens materials was accurately derived, without the use of a force sensor. An investigation into the performance and repeatability of the methods showed that the principle of optical palpation can be incorporated into OCE method to capture contact lens mechanical properties. This study shows that compression OCE combined with ‘optical palpation’ holds promise for future translation into a clinical technique to characterize the ocular tissue’s mechanical properties.

**Disclosures.** The authors declare no conflicts of interest

**Data availability.** Data underlying the results presented in this paper are not publicly available at this time but may be obtained from the authors upon reasonable request.

#### References

1. M. A. Kirby, I. Pelivanov, S. Song, L. Ambrozinski, S. J. Soon, L. Gao, D. Li, T. T. Shen, R. K. Wang, and M. O’Donnell, “Optical coherence elastography in ophthalmology,” *J. Biomed. Opt.* **22**(12), 1 (2017).
2. B. F. Kennedy, K. M. Kennedy, and D. D. Sampson, “A review of optical coherence elastography: fundamentals, techniques and prospects,” *IEEE J. Sel. Top. Quantum Electron.* **20**(2), 272–288 (2014).
3. M. Singh, J. Li, S. Vantipalli, S. Wang, Z. Han, A. Nair, S. R. Aglyamov, M. D. Twa, and L. V. Kirill, “Noncontact elastic wave imaging optical coherence elastography for evaluating changes in corneal elasticity due to crosslinking,” *IEEE J. Sel. Top. Quantum Electron.* **22**(3), 266–276 (2016).
4. M. R. Ford, W. J. Dupps, A. M. Rollins, A. S. Roy, and Z. Hu, “Method for optical coherence elastography of the cornea,” *J. Biomed. Opt.* **16**(1), 016005 (2011).
5. V. S. De Stefano, M. R. Ford, I. Seven, and W. J. Dupps, “Depth-Dependent Corneal Biomechanical Properties in Normal and Keratoconic Subjects by Optical Coherence Elastography,” *Trans. Vis. Sci. Tech.* **9**(7), 4 (2020).
6. Z. Quince, D. Alonso-Caneiro, S. A. Read, and M. J. Collins, “Static compression optical coherence elastography to measure the mechanical properties of soft contact lenses,” *Biomed. Opt. Express* **12**(4), 1821–1833 (2021).
7. K. M. Kennedy, S. Es’haghian, L. Chin, R. A. McLaughlin, D. D. Sampson, and B. F. Kennedy, “Optical palpation: optical coherence tomography-based tactile imaging using a compliant sensor,” *Opt. Lett.* **39**(10), 3014–3017 (2014).
8. K. M. Kennedy, L. Chin, R. A. McLaughlin, B. Latham, C. M. Saunders, D. D. Sampson, and B. F. Kennedy, “Quantitative micro-elastography: imaging of tissue elasticity using compression optical coherence elastography,” *Sci. Rep.* **5**(1), 15538 (2015).
9. V. Y. Zaitsev, A. L. Matveyev, L. A. Matveev, E. V. Gubarkova, A. A. Sovetsky, M. A. Sirotkina, G. V. Gelikonov, E. V. Zagaynova, N. D. Gladkova, and A. Vitkin, “Practical obstacles and their mitigation strategies in compressional optical coherence elastography of biological tissues,” *J. Innov. Opt. Health Sci.* **10**(06), 1742006 (2017).
10. K. M. Kennedy, R. Zilkens, W. M. Allen, K. Y. Foo, Q. Fang, L. Chin, R. W. Sanderson, J. Anstie, P. Wijesinghe, A. Curatolo, H. E. I. Tan, N. Morin, B. Kunjuran, C. Yeomans, S. L. Chin, H. DeJong, K. Giles, B. F. Dessauvage, B. Latham, C. M. Saunders, and B. F. Kennedy, “Diagnostic accuracy of quantitative micro-elastography for margin assessment in breast-conserving surgery,” *Cancer Res.* **80**(8), 1773–1783 (2020).
11. T. S. Bhamra and B. J. Tighe, “Mechanical properties of contact lenses: The contribution of measurement techniques and clinical feedback to 50 years of materials development,” *Contact Lens and Anterior Eye* **40**(2), 70–81 (2017).
12. P. B. Morgan, Paul J. Murphy, K. L. Gifford, P. Gifford, B. Golebiowski, L. Johnson, D. Makrynioti, A. M. Moezzi, K. Moody, M. Navasques-Cornago, H. Schweizeri, K. Swiderska, G. Young, and M. Willcox, “CLEAR-Effect of contact lens materials and designs on the anatomy and physiology of the eye,” *Contact Lens and Anterior Eye* **44**(2), 192–219 (2021).
13. D. Alonso-Caneiro, S. A. Read, and M. J. Collins, “Automatic segmentation of choroidal thickness in optical coherence tomography,” *Biomed. Opt. Express* **4**(12), 2795–2812 (2013).

14. S. J. Chiu, X. T. Li, P. Nicholas, C. A. Toth, J. A. Izatt, and S. Farsiu, "Automatic segmentation of seven retinal layers in SDOCT images congruent with expert manual segmentation," *Opt. Express* **18**(18), 19413–19428 (2010).
15. J. Tian, P. Marziliano, M. Baskaran, H.-T. Wong, and T. Aung, "Automatic anterior chamber angle assessment for HD-OCT images," *IEEE Trans. Biomed. Eng.* **58**(11), 3242–3249 (2011).
16. J. Stritzel, M. Rahlves, and B. Roth, "Refractive-index measurement and inverse correction using optical coherence tomography," *Opt. Lett.* **40**(23), 5558–5561 (2015).
17. E. Kim, M. Saha, and K. Ehrmann, "Mechanical properties of contact lens materials," *Eye & Contact Lens* **44**(2), S148–S156 (2018).
18. G. Young, R. Garofalo, S. Peters, and O. Harmer, "The effect of temperature on soft contact lens modulus and diameter," *Eye & Contact Lens* **37**(6), 337–341 (2011).
19. A. Barnes, P. H. Corkhill, and B. Tighe, "Synthetic hydrogels: 3. Hydroxyalkyl acrylate and methacrylate copolymers: surface and mechanical properties," *Polymer* **29**(12), 2191–2202 (1988).
20. J. M. Bland and D. G. Altman, "Measuring agreement in method comparison studies," *Stat Methods Med Res* **8**(2), 135–160 (1999).
21. G. Young, R. Garofalo, O. Harmer, and S. Peters, "The effect of soft contact lens care products on lens modulus," *Contact Lens and Anterior Eye* **33**(5), 210–214 (2010).
22. A. Opdahl, S. H. Kim, T. S. Koffas, C. Marmo, and G. A. Somorjai, "Surface mechanical properties of pHEMA contact lenses: viscoelastic and adhesive property changes on exposure to controlled humidity," *J. Biomed. Mater. Res.* **67A**(1), 350–356 (2003).